International Journal of GEOMATE, Jan., 2020, Vol.18, Issue 65, pp. 192-199
ISSN: 2186-2982 (P), 2186-2990 (O), Japan, DOI: https://doi.org/10.21660/2020.65.9424
Geotechnique, Construction Materials and Environment

DISCRETE ELEMENT MODEL PARAMETERS TO SIMULATE SLOPE MOVEMENTS

*Joash Bryan Adajar[1], Irene Olivia Ubay[1], Marolo Alfaro[1] and Ying Chen[2]

[1]Department of Civil Engineering, Faculty of Engineering, University of Manitoba, Canada
[2]Department of Biosystems Engineering, Faculty of Engineering, University of Manitoba, Canada

*Corresponding Author, Received: 14 June 2019, Revised: 25 Nov. 2019, Accepted: 13 Jan. 2020

ABSTRACT: Discrete Element Method (DEM) is a numerical technique that uses particulate mechanics in simulating the discontinuous behavior of particulate materials. DEM presents the advantage of modelling those materials in a particulate level allowing specifications of particle geometry including how their contacts interact. However, identifying microparameters that can accurately simulate the behavior of particulate materials is challenging. This paper presents the calibration of the microparameters of materials used in an earthfill dam that experienced slope movements. The main components of the earthfill dam under study were clay, for the core and blanket, and rockfill materials, for the protective shell. Linear parallel-bond model (LPBM) was used to describe the interactions between clay particles. Microparameters involved with the LPBM were particle stiffness, friction coefficient, bond strength, and bond stiffness. A triaxial test DEM model was developed to calibrate the clay microparameters, and it was successful in simulating the measured macroscopic peak and critical state behavior of clay materials. Rolling resistance linear model was used to describe the interactions between rockfill particles. Microparameters associated with the rolling resistance linear model were particle stiffness, friction coefficient, and rolling resistance coefficient. Large-scale direct shear test was simulated to calibrate rockfill microparameters, and it was able to capture the measured macroscopic shear behavior of rockfill materials. Calibration methodologies performed were successful in identifying appropriate microparameters for both rockfill and clay materials. The calibrated microparameters are beneficial in the development of a DEM model that can analyze movements and landslides in the vicinity of the earthfill dam or other earthfill dams built with similar materials.

Keywords: Particulate, DEM, Calibration, Dams, Landslide

1. INTRODUCTION

The discrete element method (DEM) is a numerical process that uses particulate mechanics to model the discontinuous response and behavior of particulate materials when subjected to various conditions. It simulates the mechanical behavior of a particulate system by using a collection of distinct particles that interacts with each other [1]. DEM is a useful tool for simulating physical processes that involve the separation of material constituent particles [2]. It has been used effectively in various fields like construction and building materials, agricultural, geotechnical, mining, mechanical, and industrial engineering [3–5].

The accuracy of DEM simulations is dependent on the input microparameters. A challenge that the users confront in using DEM is the identification of microparameters that define the behavior of particle interactions. There are not many laboratory tests that can quantify material microparameters. These microparameters should also be able to compensate for the simplifications made on the particle geometry used in the model [6]. One way to characterize material microparameters is through the method called *Bulk Calibration Approach* [7]. In this approach, an actual laboratory test is initially performed to measure a particular material macroscopic (bulk) property. Subsequently, a DEM model of the laboratory test is developed, and sensitivity analysis is performed to see how the microparameters influence its results. A calibration approach is then designed based on the observed influence of the microparameters to systematically adjust the microparameter values and match the measured and simulated macroscopic material property.

This paper presents the calibration of microparameters of the components of a particular earthfill dam that experienced slope movements [8]. The main components of the earthfill dam are clay, for the clay core and blanket, and rockfill materials, as protective shell. This paper also intends to identify how each microprameter affects the macroscopic behavior of the materials. Identifying the effects of the microparameters can help in correlating the micromechanical and macromechanical material properties. Clay and rockfill microparameters are beneficial in developing DEM models that can analyze the behavior of the past landslide that has occurred and potential landslides that may occur in similar earthfill dams.

2. CLAY MICROPARAMETERS

2.1 Triaxial Test

Undrained consolidated triaxial tests were performed on the clay samples, classified as lacustrine clay of high plasticity, collected from the earthfill dam. The preconsolidation pressure considered for the test was 400 kPa, and it was sheared with overconsolidation ratios of 4, 2, and 1. The results were analyzed using the concept of Critical State Soil Mechanics (CSSM). The monitored results during the test were the relationships between deviatoric stress (q) and axial strain (ε_1), and deviatoric stress (q) and mean effective stress (p'). The measured peak and critical state friction angles were 24° and 18.4°, respectively.

2.2 Discrete Element Model

2.1.1 Model Development

The material vessel for the triaxial test was modelled using three walls: one cylindrical wall and two disk walls. The purpose of the cylindrical wall was to radially confine the particles and compress it with a particular pressure. The set diameter of the cylindrical wall was 71 mm, and it simulates the existence of the rubber membrane that envelopes the sample in the actual test. The two disks simulate the upper and lower platen of the triaxial test equipment. They confine the material vertically and are capable of moving at a particular speed to shear the material. The set distance between the two disks was 142 mm. The dimensions set were identical to the initial geometry of the actual clay sample before testing.

The clay sample was modelled using spherical particles with a diameter of 5 mm. Nandanwar and Chen [9] used the same particle size and shape for the microparameter calibration of cohesive soils tested with triaxial test. A total number of 5,155 particles were observed to be enough to fill the volume of the material vessel. Particles were positioned inside the material vessel through gravity deposition method [3]. In the gravity deposition method, generated particles were let to fall inside the material vessel with the effect of gravitational acceleration (9.8 m/s^2). The assigned particle density was calculated by matching the measured and simulated initial bulk density of the material. The model was then cycled until it reaches an equilibrium state. The material vessel and clay particles generated for the triaxial test DEM model are shown in Fig. 1.

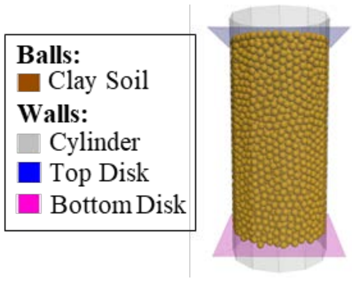

Fig. 1 Triaxial test DEM model

2.1.2 Triaxial Test Simulation

Three phases are involved in the undrained consolidated triaxial test: the preconsolidation phase, consolidation phase, and shearing phase. A pressure-controlled (*servo* mechanism) boundary condition was designated on the cylindrical and disk walls to isotropically consolidate the sample with the desired pressure during the preconsolidation phase. Preconsolidation pressure considered for the model was the same as the actual triaxial test, which is 400 kPa. After the preconsolidation pressure was observed to equilibrate, the consolidation phase was initiated by assigning an equal or lower pressure value depending on the considered overconsolidation ratio (OCR): 100 kPa for an OCR of 4; 200 kPa for an OCR of 2; and 400 kPa for an OCR of 1.

For the shearing phase, the volumetric strain should be zero (constant-volume) in an undrained consolidated triaxial test. To initiate the shearing phase and simulate this constant-volume condition, a strain-controlled boundary condition was assigned on the three walls [10].

Similar relationships (q vs ε_1 and q vs p') obtained from the actual triaxial test were monitored in the model.

2.1.3 Model Parameters

The linear parallel-bond model (LPBM) was selected to simulate the interactions between clay particles. The behavior of a cohesive soil can be efficiently captured by the linear parallel-bond model [9]. The microparameters associated with the linear parallel-bond model are friction coefficient (μ), particle normal stiffness (k_n), particle shear stiffness (k_s), bond normal stiffness ($\bar{k}_n$), bond shear stiffness ($\bar{k}_s$), bond tensile strength ($\bar{\sigma}_c$), and bond cohesive strength ($\bar{c}$). In an attempt to minimize the number of microparameters to be calibrated, the normal and shear components of the microparameters are assumed to be equal [11]. Hereafter, particle normal and shear stiffness will be called particle stiffness (k), bond normal and shear stiffness as bond stiffness ($\bar{k}$), and lastly, bond tensile and cohesive strength as bond strength ($\bar{c}$). Consequently, there are a total of four microparameters to be calibrated in order to simulate the actual behavior of the clay sample: k, μ, $\bar{k}$, and $\bar{c}$.

2.1.4 *Sensitivity Analyses and Calibration*

Sensitivity analyses were performed to identify the sensitivity of the equivalent macroscopic shear behavior of the numerical material model to the linear parallel-bond microparameters — k, μ, $\bar{k}$, and $\bar{c}$. The governing peak stress (q_p) and critical state stress (q_{cs}) observed from the macroscopic stress-strain relationships were specifically examined during the sensitivity analysis. The consolidation pressure considered for the sensitivity analysis was the mid-range value (200 kPa) among the consolidation pressures used in the actual test. The results of the sensitivity analysis were used as the basis for the design of a systematic calibration approach for the linear parallel-bond microparameters in order to simulate the real behavior of the clay samples.

Figure 2 shows the results of the sensitivity analysis when particle stiffness was varied. It shows the changes in the development of the macroscopic stress-strain relationships. Varying the particle stiffness value did not introduce the occurrence of peak stress at low strains. At high particle stiffness values (7.5e4 – 10e4 N/m), the material model appeared not to reach a critical state (constant deviatoric stress at high shear strain) as deviatoric stress continues to increase even at 15% shear strain. Hence, in these instances, to avoid confusion on the comparisons made on the critical state stress, the critical state stress considered was the deviatoric stress simulated at 15% shear strain (end of test). From the graphs, the particle stiffness was mainly influential on the critical state stress, wherein an increase in its value results to an increase in the critical state stress.

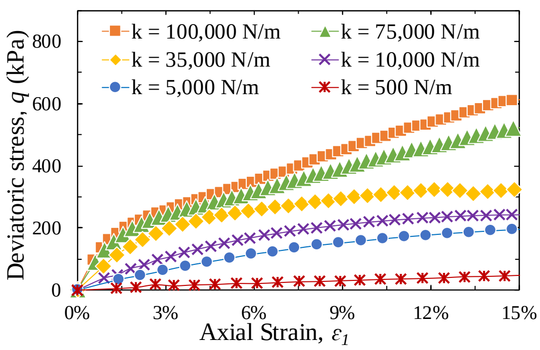

Fig. 2 Influence of particle stiffness on the stress-strain relationship of clay

The friction coefficient mainly affects the critical state stress (Fig. 3). The observed trend was that an increase in the friction coefficient was accompanied by an increase in the resulting critical state stress. The model did not exhibit the incidence of a peak stress, while the manifestation of material critical state was evident in the entirety of the range of friction coefficient values considered for the sensitivity analysis.

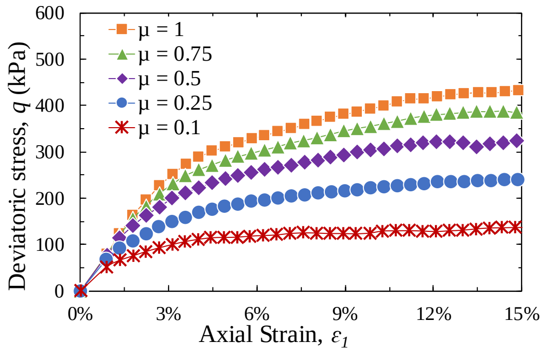

Fig. 3 Influence of particle friction coefficient on the stress-strain relationship of clay

Both the parallel-bond microparameters, bond strength and bond stiffness, were observed to primarily affect the clay peak stress behavior. The influence of bond strength on the clay stress-strain relationships is shown in Fig. 4. The effect of bond strength is more apparent on the peak stress than the critical state stress. However, there is a bond strength threshold value (200 kPa) that needs to be exceeded for the peak behavior to manifest. Once the threshold value is exceeded, an increase in the peak stress can be observed as the bond strength is increased. Choosing bond strengths lower than the threshold value results for the parallel-bond microparameters to be non-influential on the stress-strain behavior because of the immediate breakage of the bonds.

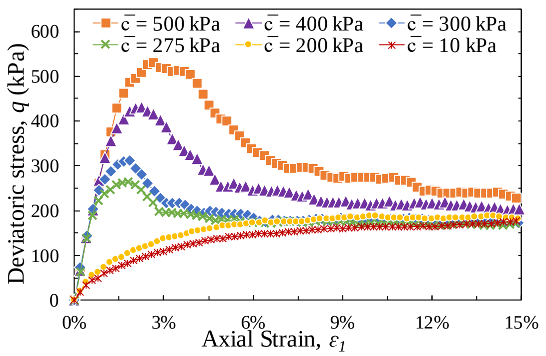

Fig. 4 Influence of bond strength on the stress-strain relationship of clay

The bond stiffness is inversely related to the peak stress (Fig. 5). Earlier breakage of the bonds can be observed if high bond stiffness (3e9 – 5e10 Pa/m) is chosen, which results in a low peak stress value. The material model behaves like a brittle material when high bond stiffness is used. On the other hand, at low bond stiffness (5e7 Pa/m), the bonds tend to not break at all because it becomes extremely flexible and minimal stresses develop within the bonds even at higher strains; that is why the deviatoric stress continuously increase. When the bonds break, the material simply behaves like an unbonded material where the governing microparameters are only the friction coefficient and particle stiffness.

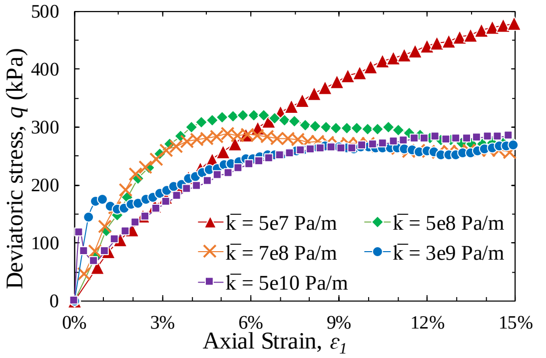

Fig. 5 Influence of bond stiffness on the stress-strain relationship of clay

To summarize, the behavior in the range where peak stress generally occurs (low strains) is dictated by the additional shear resistance provided by the bond strength and bond stiffness. While in the critical state domain, clay particle interactions are controlled by the particle stiffness and friction coefficient. This is the reason why the critical state stress has almost similar values despite varying the parallel-bond microparameters ($\bar{k}$ and $\bar{c}$). The slight variations on the critical state domain observed when changing the values of the parallel-bond microparameters are due to some of the bonds that were not broken.

From the results of the sensitivity analysis, it was concluded that the best approach to match the measured results was to focus the calibration of the parallel-bond microparameters in matching the actual peak stress, while particle stiffness and friction coefficient was calibrated to match the actual critical state stress. After executing this calibration approach, the back-calculated microparameters are listed in Table 1.

Table 1 Clay microparameter values

Parameters	Value	Units
Particle Stiffness (k)	3.5e4	N/m
Friction (μ)	0.15	—
Bond Stiffness ($\bar{k}$)	1e9	Pa/m
Bond Strength ($\bar{c}$)	1.1e5	Pa

2.2 Results

The triaxial test model, integrated with the calibrated microparameters, was found to be predictive as it was able to simulate the actual clay behavior at different consolidation pressures (100, 200, 400 kPa). Good agreement can be observed on the measured and simulated stress-strain (q vs ε_1) relationships as shown in Fig. 6. Also, good comparison can be made between the measured and simulated critical state and peak strengths identified from the q vs p' graphs where the corresponding critical state and peak lines can also be observed (Fig. 7). Using the concept of Critical State Soil Mechanics (CSSM), the simulated critical state and peak friction angles were calculated. In comparing them with the measured critical state and peak friction angles, there are only minimal differences which are about 0.9° to 1.1° (Table 2).

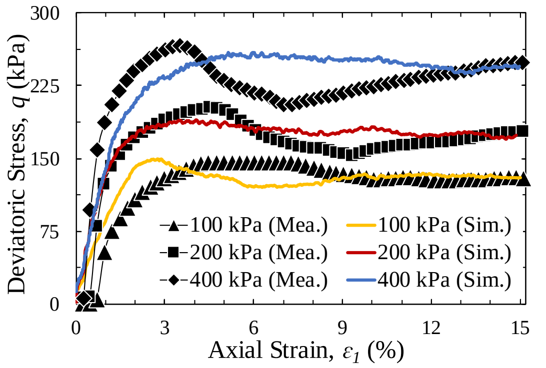

Fig. 6 Measured and simulated stress-strain relationships of clay

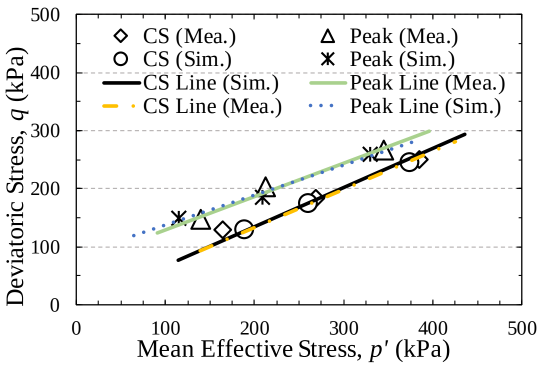

Fig. 7 Measured and simulated critical-state and peak strengths

Table 2 Critical state and peak friction angles

Parameter	Peak		Critical state	
	Mea.	Sim.	Mea.	Sim.
Friction Angle	24°	25.1°	18.4°	17.5°

3. ROCKFILL MICROPARAMETERS

2.3 Large-scale Direct Shear Test

Information on the macroscopic behavior of rockfill materials was obtained from literature. Alfaro et al. [12] carried out experimental testing using a large-scale direct shear box, which has a diameter of 600 mm and overall specimen height of 420 mm, to measure and observe the mobilization of shear strength of rockfill materials. Rockfill materials were tested under three different normal pressures (50, 75, and 100 kPa). It was sheared up until 30 mm, which is around 5% shear strain. The stress-strain relationships obtained from the large-scale direct shear tests were used as the basis in calibrating the microparameters for rockfill.

2.4 Discrete Element Model

3.1.1 *Model Development*

Four walls were used to model the large-scale direct shear box: two cylindrical and two disk walls. The diameter of the cylinders was 600 mm. The height of the upper cylinder was 150 mm, while the lower cylinder was 270 mm. Dimensions set were the same as the actual equipment. The two cylindrical walls were used as horizontal enclosures to represent the top and bottom shear boxes, while the two disk walls vertically confined the material to represent the bottom and top caps. A friction coefficient of 0 was assigned on the cylindrical walls to simulate the smooth sidewalls of the shear box.

Spherical particles, having a uniform particle size of 25 mm diameter, were generated to represent the rockfill particles. Particle size considered was comparable to the particle size in the actual test but the actual angular (non-spherical) shape of the particles is difficult to model. A microparameter will be introduced later to account for the effects of the angularity of particles on the behavior of the rockfill. Gravity deposition method was the packing methodology followed to position the particles inside the shear box [3]. There are a total of 8,317 particles inside the large-scale shear box. The DEM model of the large-scale direct shear box and rockfill particles is shown in Fig. 8.

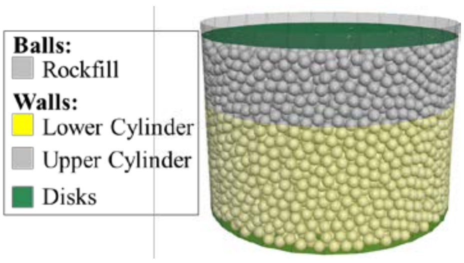

Fig. 8 Large-scale direct shear test DEM model.

3.1.2 Direct Shear Test Simulation

The direct shear test model involves two phases: the compression phase and shearing phase. For the compression phase, a pressure-controlled boundary condition was assigned on the top disk to compress the particles with the designated normal pressure. The compression phase ends once the normal pressure stabilizes and there are no succeeding vertical displacements observed on the material.

For the shearing phase, it was initiated by moving the bottom cylinder and disk to the right. The material model was sheared up to 5% shear strain, similar to the actual test.

The shear stress experienced by the material was tracked during the shearing phase, and the corresponding stress-strain relationships were monitored for each test simulations.

3.1.3 Model Parameters

Rolling resistance linear model was used to represent the contact behavior of the rockfill particles. The microparameters associated with the rolling resistance linear model are particle stiffness (k, $k_n = k_s$), friction coefficient (μ), and rolling resistance coefficient (μ_r). Particle shear and normal stiffness were again assumed to be equal to decrease the number of microparameters to be calibrated. The μ_r was introduced to represent the angular nature of rockfill materials and to simulate its effect on the rolling motion of the particles in the model [13]. μ_r is significant in modelling materials of high shearing resistance because the effects of the angularity of the real particle shape and roughness of particle surface are hard to mimic when spherical particles are used for the model [14].

3.1.4 Sensitivity Analyses and Calibration

Sensitivity analyses were performed to identify the influence of the microparameters — particle stiffness, friction coefficient, and rolling resistance coefficient — on the progression (shear stiffness) of the macroscopic stress-strain relationships and on the governing shear stress at the end of the test (5% shear strain). From here on, the governing shear stress at 5% shear strain will be called “end shear strength”. The end shear strength was arbitrarily monitored because in the work of Alfaro et al. [12], the material was only shear up to 5% shear strain. The normal pressure considered was the mid-range value (75 kPa) of the three normal pressures chosen for the actual test.

Figure 9 shows the sensitivity of the stress-strain relationship on friction coefficient. It can be observed that the friction coefficient does not significantly affect the material shear stiffness during the early stages of shearing (up to 1.5% strain). However, the increase in the end shear strength was prominent as the friction coefficient is increased.

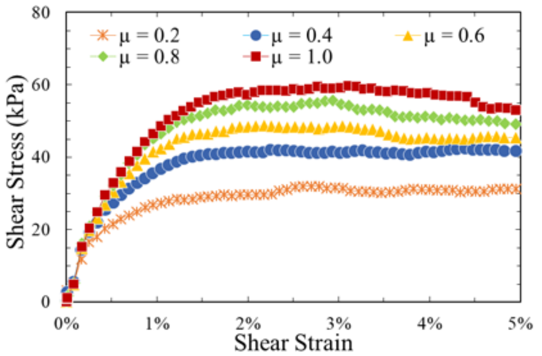

Fig. 9 Influence of friction coefficient on the stress-strain relationship of rockfill.

Particles stiffness dictates the resulting material shear stiffness (Fig. 10). As the value of particle stiffness increases, an overall stiffer material response was observed, and the manifestation of the critical state occurs at lower strains. When low particle stiffness (5e4 – 1e5 N/m) was used, there were instances when material critical state was not even reached; this finding is significant as it was observed from the actual test that critical state did not manifest when rockfill materials were sheared up to 5% shear strain. It was also observed that an increase in particle stiffness increases the governing end shear strength. Another significant observation was that particle stiffness becomes less influential on the model results as its value increases.

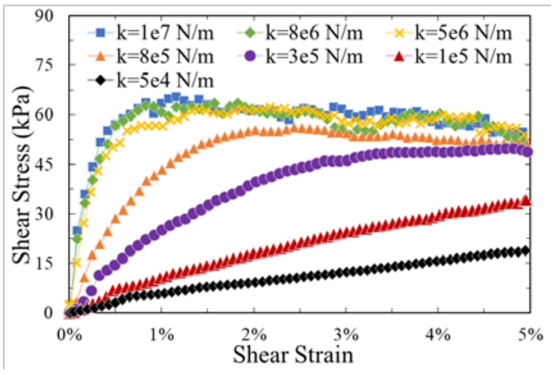

Fig. 10 Influence of particle stiffness on the stress-strain relationship of rockfill.

Rolling resistance coefficient was observed to increase the end shear strength but does not significantly affect the material shear stiffness (Fig. 11). Similar to particle stiffness, it also becomes less influential to the model as its value increases.

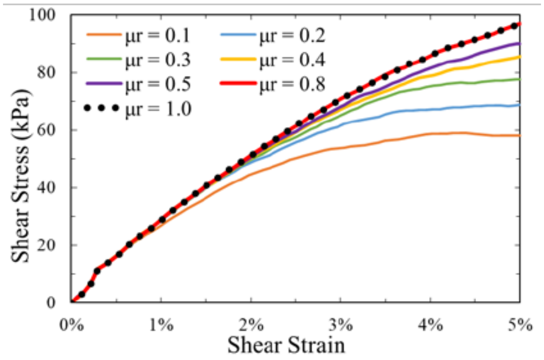

Fig. 11 Influence of rolling resistance coefficient on the stress-strain relationship of rockfill.

For the calibration process, the initial methodology followed was to focus on the calibration of particle stiffness and friction coefficient. Particle stiffness was mainly adjusted to match the macroscopic shear stiffness, while friction coefficient was mainly adjusted to match the end shear strength. Upon the execution of a couple of simulations, it was observed that it is possible to match the macroscopic shear stiffness by adjusting the particle stiffness. However, given that particular particle stiffness, the end shear strength is difficult to match by only adjusting the friction coefficient. Despite increasing the friction coefficient to 1, the model still cannot simulate the actual end shear strength. Hence, the rolling resistance coefficient was introduced to provide additional shear resistance and increase the end shear strength without significantly altering the material shear stiffness. After the calibration process, the microparameter values that can best simulate the actual stress-strain behavior of rockfill materials are listed in Table 3.

Table 3 Rockfill microparameter values

Parameters	Value	Units
Particle Stiffness (k)	3e5	N/m
Friction (μ)	1	—
Rolling Resistance (μ_r)	0.2	—

3.3 Results

The measured and simulated stress-strain relationships for all the normal pressures (50, 75, and 100 kPa) considered for the test were in good agreement (Fig. 12). Table 4 shows the measured and simulated shear strengths at the end of the test (5% shear strain) where minimal differences can be observed, which only range from 1.4 to 6 kPa (less than 5% relative error).

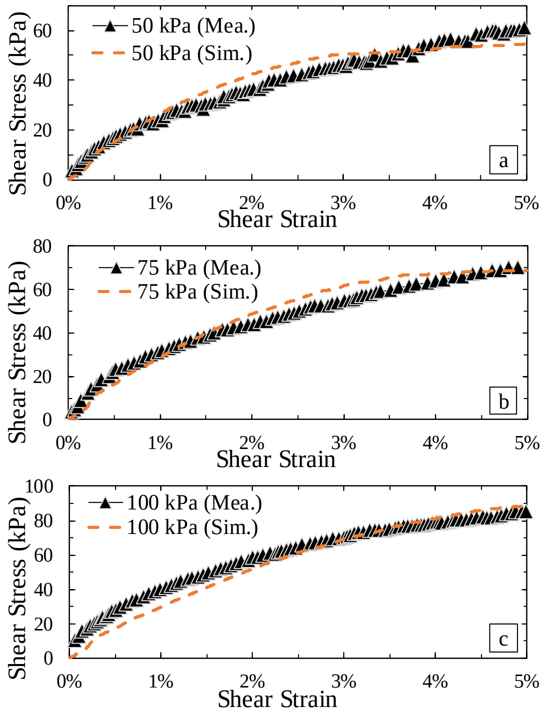

Fig. 12 Measured and simulated stress-strain relationships of rockfill at different confining pressures: a. 50 kPa, b. 75 kPa and c. 100 kPa.

Table 4 Measured and simulated rockfill shear strength at 5% shear strain.

Normal Pressure (kPa)	Shear strength (kPa) at 5% shear strain	
	Measured	Simulated
50	61	55
75	70.2	68.8
100	87.6	85.5

4. SLOPE MOVEMENT IN AN EARTHFILL DAM

The clay and rockfill microparameters can be used to aid in the development of a landslide DEM model that can simulate the observed movements at the slope of an earthfill dam. An example of a landslide model developed using the calibrated microparameters is shown in Fig. 13. It displays the z-displacement (m) contour where depression and bulging on the dam crest and toe, respectively, can be observed. The landslide model was successfully validated and was able to simulate the post-landslide morphology of an earthfill dam located in Ontario, Canada. This provides confidence in the use of landslide DEM models with input microparameters calibrated from the laboratory tests considered in this paper. The model can be used to simulate potential future landslides on similar earthfill dams, which can give researchers insights on the behavior of the soil flow. Information on the displacements and velocities of different portions of the moving soil mass can be extracted from the model. This information is helpful in the design of landslide mitigation structures and in hazard mapping the surroundings of the earthfill dam.

5. CONCLUSIONS

There are different methods that can be used to calibrate material microparameters. The use of triaxial and direct shear test simulations for microparameter calibration purposes has been found to be effective in this research. Linear parallel bond microparameters were successfully calibrated for clay, while rolling resistance linear model microparameters were successfully calibrated for rockfill. The laboratory test DEM models were able to simulate the macroscopic behavior of the materials, which were obtained from actual laboratory tests. The triaxial test model was able to capture the critical state and peak behavior of clay,

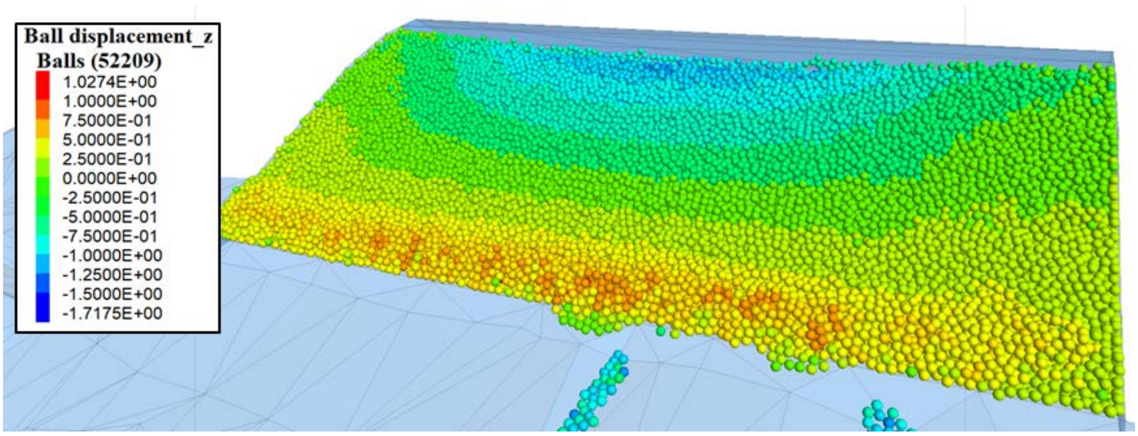

Fig. 13 Z-displacement contour from the landslide DEM model of the earthfill dam.

while the direct shear test model was able to simulate the shear behavior of rockfill materials.

From the calibration methodologies performed, it can be observed that the influence of microparameters is complicated. The influence of the contact model microparameters varies for different laboratory tests. For the influence of linear parallel-bond model microparameters on the results of the triaxial test model, parallel-bond microparameters ($\bar{c}$ and $\bar{k}$) were observed to dictate the material behavior at lows strains (peak domain), while particle stiffness and friction coefficient dictate the material behavior at high strains (critical state domain). For the influence of rolling resistance linear model microparameters on the results of the direct shear test model, friction and rolling resistance coefficients dictate the resulting end shear strength, while particle stiffness mainly affects the material shear stiffness. It is recommended to perform sensitivity analysis and design a calibration approach based on the results.

The developed landslide DEM model highlighted the applicability of the calibrated clay and rockfill microparameters on a broader research that involves large-scale physical processes. The successful validation of the landslide model reaffirmed that the calibration approach followed in this research can reasonably characterize microparameters that improved the reliability of the landslide model. The microparameters can be used in developing landslide models for the other sections of the earthfill dam or other earthfill dams built with similar materials

Identified microparameters in this research should be used with caution. It is important to take note that characterized microparameters are considered as apparent microparameters which are only applicable to material models having identical conditions as what was presented in this research. Differences in model behavior may be observed upon the use of different particle geometry and distributions.

6. ACKNOWLEDGMENTS

This research was funded by the Natural Sciences and Engineering Research Council of Canada (NSERC).

7. REFERENCES

[1] Cundall P.A. and O. D. L. Strack, A Discrete Numerical Model For Granular Assemblies, Geotechnique, Vol. 29, No. 1, 1979, pp. 47–65.

[2] Mei C.J., Determination Of Microparameters For Discrete Element Modelling Of Granular Materials With Varying Particle Size Using One-Dimensional Compression Testing, Masters Thesis. University of British Columbia, 2017.

[3] Ahlinhan M.F., Ernesto H., Marius B.K., Valery D., Quirin A., Nicholas S. and Edmond A., Experiments And 3D DEM Of Triaxial Compression Tests Under Special Consideration Of Particle Stiffness, Geomaterials, Vol. 08, No. 04, 2018, pp. 39–62.

[4] Obermayr M., C. Vrettos, and P. Eberhard, A Discrete Element Model For Cohesive Soil, III Int. Conf. Part. Methods - Fundam. Appl., No. September 2013, 2013, pp. 783–794.

[5] Zeng Z. and Y. Chen, Simulation Of Straw Movement By Discrete Element Modelling Of Straw-Sweep-Soil Interaction, Biosyst. Eng., Vol. 180, 2019, pp. 25–35.

[6] Shmulevich I., Chapter 5. Discrete Element Modeling Of Soil-Machine Interactions, Adv. Soil Dyn., Vol. 3, 2009, pp. 399–433.

[7] Coetzee C.J., Review: Calibration Of The Discrete Element Method, Powder Technol., Vol. 310, 2017, pp. 104–142.

[8] Ubay I.O. and M. Alfaro, Numerical Modelling Of A Clay Core Earth Fill Dam With And Without Creep Deformation, in Canadian Geotechnical Conferece (GeoSt.John's), 2019.

[9] Nandanwar M. and Y. Chen, Modeling And Measurements Of Triaxial Tests For A Sandy Loam Soil, Can. Biosyst. Eng., Vol. 59, No. 1, 2017, pp. 2.1-2.8.

[10] Sitharam T., Evaluation Of Undrained Response From Drained Triaxial Shear Tests : DEM Simulations And Experiments, Geotechnique, Vol. 58, No. 7, 2008, pp. 605–608.

[11] Sadek M. and Y. Chen, Feasibility Of Using PFC3D To Simulate Soil Flow Resulting From A Simple Soil-Engaging Tool, Trans. ASABE, Vol. 58, No. 4, 2015, pp. 987–996.

[12] Alfaro M.C., J. a. Blatz, W. F. Abdulrazaq, and C.-S. Kim, Evaluating Shear Mobilization In Rockfill Columns Used For Riverbank Stabilization, Can. Geotech. J., Vol. 46, No. 8, 2009, pp. 976–986.

[13] Ai J., J. F. Chen, J. M. Rotter, and J. Y. Ooi, Assessment Of Rolling Resistance Models In Discrete Element Simulations, Powder Technol., Vol. 206, No. 3, 2011, pp. 269–282.

[14] Belheine N., J. P. Plassiard, F. V. Donzé, F. Darve, and A. Seridi, Numerical Simulation Of Drained Triaxial Test Using 3D Discrete Element Modeling, Comput. Geotech., Vol. 36, No. 1–2, 2009, pp. 320–331.